AIP | Physics of Plasmas

Coupled nonlinear drift and ion acoustic waves in dense dissipative electron-positron-ion magnetoplasmas

W. Masood, S. Karim, H. A. Shah, and M. Siddiq

Citation: Physics of Plasmas (1994-present) **16**, 112302 (2009); doi: 10.1063/1.3253623
View online: http://dx.doi.org/10.1063/1.3253623
View Table of Contents: http://scitation.aip.org/content/aip/journal/pop/16/11?ver=pdfcov
Published by the AIP Publishing

Coupled nonlinear drift and ion acoustic waves in dense dissipative electron-positron-ion magnetoplasmas

W. Masood,[1] S. Karim,[2] H. A. Shah,[2] and M. Siddiq[1]
[1]*TPPD, PINSTECH, P.O. Nilore, 44000 Islamabad, Pakistan*
[2]*Department of Physics, GC University, 54000 Lahore, Pakistan*

(Received 4 May 2009; accepted 30 September 2009; published online 4 November 2009)

Linear and nonlinear propagation characteristics of drift ion acoustic waves are investigated in an inhomogeneous electron-positron-ion (e-p-i) quantum magnetoplasma with neutrals in the background using the well known quantum hydrodynamic model. In this regard, Korteweg–de Vries–Burgers (KdVB) and Kadomtsev–Petviashvili–Burgers (KPB) equations are obtained. Furthermore, the solutions of KdVB and KPB equations are presented by using the tangent hyperbolic (tanh) method. The variation in the shock profile with the quantum Bohm potential, collision frequency, and the ratio of drift to shock velocity in the comoving frame, v_*/u, is also investigated. It is found that increasing the positron concentration and collision frequency decreases the strength of the shock. It is also shown that when the localized structure propagates with velocity greater than the diamagnetic drift velocity (i.e., $u > v_*$), the shock strength decreases. However, the shock strength is observed to increase when the localized structure propagates with velocity less than that of drift velocity (i.e., $u < v_*$). The relevance of the present investigation with regard to dense astrophysical environments is also pointed out. © *2009 American Institute of Physics*.
[doi:10.1063/1.3253623]

I. INTRODUCTION

The field of quantum plasmas has grown tremendously in the past couple of years owing to its wide range of applicability in numerous situations of interest such as in microelectronic devices,[1] in dense astrophysical environments[2,3] (for instance, white dwarfs and neutron stars), in high intensity laser produced plasmas,[4] as well as in dusty plasmas.[5–7] Traditional plasma physics deals with the study of regimes that are characterized by low density and high temperatures where the quantum effects are negligibly small. However, in the systems mentioned above, the importance of quantum effects has been acknowledged. When quantum effects begin to play a role, an additional scale length is introduced, namely, the de Broglie wavelength of the charged species, $\lambda_B = h/(2\pi m v_T)$. It roughly represents the spatial extent of the particle wave function—the larger it is, the more pronounced these effects are.

The two mathematical formulations that have been frequently employed in quantum plasmas are the Wigner–Poisson and the Schrödinger–Poisson, respectively. These two approaches are generally employed to describe the statistical and hydrodynamic behavior of charged species at quantum scales in dense plasmas. These two approaches are the quantum analogs of kinetic and fluid treatments of classical plasmas, respectively. The two approaches have been expounded in detail by Manfredi.[8] The quantum hydrodynamic (QHD) model is based on the Schrödinger–Poisson formulation. It has been extensively used to study the linear and nonlinear propagation characteristics of several waves in the quantum plasmas.[6,7,9,10] The benefits of the QHD model rest in its simplicity, numerical efficiency, the direct use of macroscopic variables of interest such as energy and momentum, and the ease with which the boundary conditions are implemented. The major shortcoming of the QHD model is that the velocity space effects such as Landau damping cannot be studied in its realm as the QHD equations are obtained by taking the moments of the Wigner distribution function.[11]

The QHD model has also been used to study the propagation of linear and nonlinear waves in inhomogeneous quantum plasmas. El-Taibany and Wadati[11] studied the dynamics of nonlinear quantum dust acoustic wave in a nonuniform quantum dusty plasma and found that the formation of solitons manifested a dependence on a critical value of plasma parameters unlike a homogeneous plasma. Shukla and Stenflo[12] found new drift modes in nonuniform quantum magnetoplasmas and observed that the Bohm potential term significantly modified the electron drift wave frequency. Wu *et al.*[13] studied the electrostatic drift vortices in quantum magnetoplasmas employing the QHD model and found that the waves got modified significantly by the quantum corrections. Masood *et al.*[14] investigated quantum ion acoustic vortices in an inhomogeneous plasma and found that electrostatic monopolar, dipolar, and vortex street type solutions could appear in such a plasma. It was observed that the inclusion of the quantum statistical and Bohm potential terms appreciably modified the scale lengths of these structures.

Electron-positron plasmas have been observed to behave differently as opposed to the typical electron-ion (e-i) plasmas.[15,16] An interesting feature of electron-positron (e-p) plasma by comparison with the usual electron-ion plasma is the same mass and equal magnitude of charge of the components of an e-p plasma. Electron-positron plasmas have been observed in active galactic nuclei,[17] in pulsar magnetospheres,[18] in the polar regions of neutron stars,[19] as well as in the intense laser fields.[20] Electron-positron plasmas are also believed to have existed in the early universe[21] and are also present at the center of our own galaxy.[22] Electron-positron-ion plasmas have also been a subject of investigation in quantum plasmas. Ali *et al.*[10] studied the linear and nonlinear ion acoustic waves in an unmagnetized electron-positron-ion (e-p-i) quantum plasma. The authors derived the Korteweg–de Vries equation for quantum e-p-i plasma and an energy equation for arbitrary amplitude ion acoustic waves and discussed the relevance of their results. Khan and Masood[23] investigated quantum ion acoustic wave propagation in a magnetized e-p-i plasma and found that the structure of the ion acoustic soliton depended on the quantum pressure, concentration of positrons, strength of magnetic field, and the angle of propagation. Masood *et al.*[24] studied the propagation of quantum ion acoustic shock waves in planar and nonplanar geometries and found that the strength of the shock was maximum for spherical and minimum for the planar geometry. It was also found that the increase in quantum Bohm potential decreased the strength of the quantum ion acoustic shock waves. Sabry *et al.*[25] investigated the propagation of ion acoustic envelope solitary waves in dense e-p-i plasmas and found that such a plasma was modulationally unstable for nonplanar geometry that had no counterpart in planar geometry. Haque *et al.*[26] studied the linear and nonlinear drift waves in inhomogeneous quantum plasmas with neutrals in the background in e-p-i plasmas and found that the positron concentration and quantum corrections appreciably modified the drift solitons and shocks in quantum magnetoplasmas. Recently, Ren *et al.*[27] studied the linear electromagnetic drift waves in nonuniform quantum e-p-i magnetoplasma employing the QHD model and applied their results in the dense astrophysical environments.

It is a well established fact that shock waves can be excited in a dissipative nonlinear medium. There can be several dissipative processes in a plasma. The important ones include Landau damping, kinematic viscosity among the plasma constituents, as well as collisions between charged particles and neutrals present in the system. However, when a medium has both dispersive and dissipative properties, the propagation of small amplitude perturbations can then be adequately described by Korteweg–de Vries–Burgers (KdVB) equation. The dissipative term (i.e., the Burgers term) in the KdVB equation arises by taking into account the kinematic viscosity among the plasma constituents.[28–30] When wave breaking due to nonlinearity is balanced by the combined effect of dispersion and dissipation, a monotonic or oscillatory dispersive shock wave is generated in a plasma.[30–33] It is well known that transverse perturbations would always exist in the higher dimensional system. The inclusion of transverse perturbation introduces an anisotropy in the system, which modifies the wave structure and the stability of the system.[34,35] In this paper, shock propagation in the presence of parallel perturbation is considered in an inhomogeneous electron-positron-ion (e-p-i) quantum magnetoplasma.

In this paper, coupling of nonlinear drift and ion acoustic waves in dissipative dense e-p-i magnetoplasmas is investigated. In this regard, both quantum KdVB and Kadomtsev–Petviashvili–Burgers (KPB) equations are derived and their solutions are given using the tanh method. The dissipative effect appears due to the collisions of the ions with the neutrals in the background. This paper is organized as follows. In Sec. II, we present the basic set of nonlinear equations for the system under consideration. In Sec. III, linear dispersion relation of the quantum ion acoustic wave in an inhomogeneous quantum magnetoplasma is presented and different limiting cases are also discussed. In Secs. IV and V, nonlinear KdVB and KPB equations are derived and their solutions are given by using the tanh method. Stability analysis of KPB is presented in Sec. VI. In Sec. VII, results are presented and discussed. Finally, in Sec. VIII, the conclusion of the current investigation is presented.

II. GOVERNING EQUATIONS

Consider an inhomogeneous quantum magnetoplasma composed of electrons, positrons, and ions with neutrals in the background. The equilibrium magnetic field is in the z-direction, i.e., $\mathbf{B}_0=\hat{\mathbf{z}}B_0$, whereas the density and temperature gradients are assumed to be in the negative x-direction, i.e., $\boldsymbol{\nabla} n_{j_0}=-\hat{\mathbf{x}}\partial_x n_{j_0}$ and $\boldsymbol{\nabla} T_{F_{j_0}}=-\hat{\mathbf{x}}\partial_x T_{F_{j_0}}$. The phase velocity of the wave is assumed to be $v_{Fi}\ll\omega/k\ll v_{Fe}, v_{Fp}$ (v_{Fi}, v_{Fe}, and v_{Fp} are the ion, electron, and positron Fermi velocities, respectively). We, therefore, ignore the quantum pressure and Bohm potential contributions of ions. Using the QHD model, we can write down the governing equations as follows.

The equation of motion for electrons and positrons is

$$m_j n_j\left(\frac{\partial}{\partial t}+\mathbf{v}_j\,.\,\boldsymbol{\nabla}\right)\mathbf{v}_j=q_j n_j\left(\mathbf{E}+\frac{1}{c}\mathbf{v}_j\times\mathbf{B}_0\right)-\boldsymbol{\nabla} p_j+\frac{\hbar^2 n_j}{2m_j}\boldsymbol{\nabla}\left(\frac{\nabla^2\sqrt{n_j}}{\sqrt{n_j}}\right),\qquad(1)$$

where $j=e$ (electron) and p (positron), $q_j=(-c,+c)$ for electron and positron, $E=-\nabla\phi$ is the electrostatic field (ϕ is electrostatic potential), $\hbar=h/2\pi$ (h is Planck's constant), and m_e, n_e, and e are the electron mass, density, and charge, respectively. In Eq. (1), two different quantum effects, i.e., the quantum diffraction (due to Bohm potential) and quantum statistical pressure (due to Fermi–Dirac distribution), are included.

The electron and positron pressures are defined as[36]

$$p_j=\frac{\hbar^2}{5m_j}(3\pi^2)^{2/3}n_j^{5/3}.\qquad(2)$$

The parallel component of Eq. (1) for inertialess electrons gives

$$e\partial_z\phi-\frac{1}{n_e}\partial_z p_e+\frac{\hbar^2}{2m_e}\partial_z\left(\frac{\nabla^2\sqrt{n_e}}{\sqrt{n_e}}\right)=0\qquad(3)$$

using the pressure given in Eq. (2). Integrating Eq. (3) and using boundary conditions $n_e=n_{e_0}$, and $\phi=0$ at $z\to\pm\infty$, expanding Eq. (3) by Taylor series, and assuming that the Bohm potential term is small, Eq. (3) after back substitution can be written as[37]

$$\left(\frac{\widetilde{n_e}}{n_{e_0}}\right)=\frac{3e\phi}{2k_BT_{Fe}}+\frac{3e^2\phi^2}{8k_B^2T_{Fe}^2}+\frac{9e\hbar^2}{16m_ek_B^2T_{Fe}^2}\nabla^2\phi, \quad (4)$$

where $\widetilde{n_e}$ is the perturbed electron density, while n_{e_0} is the equilibrium density and $\widetilde{n_e} < n_{e_0}$. Similarly, for positrons, we have

$$\left(\frac{\widetilde{n_p}}{n_{p_0}}\right)=-\frac{3e\phi}{2k_BT_{Fp}}+\frac{3e^2\phi^2}{8k_B^2T_{Fp}^2}-\frac{9e\hbar^2}{16m_pk_B^2T_{Fp}^2}\nabla^2\phi, \quad (5)$$

where k_B is the Boltzmann constant and $T_{F_j}=[\hbar^2(3\pi^2)^{2/3}n_j^{2/3}/2m_jk_B]$ is the Fermi temperature for either species $(j=e,p)$.

The equation of motion for ions is

$$m_in_i(\partial_t+\mathbf{v}_i\cdot\nabla)\mathbf{v}_i=en_i\left(\mathbf{E}+\frac{1}{c}\mathbf{v}_i\times\mathbf{B}_0\right)-m_in_i\nu_{in}\mathbf{v}_i, \quad (6)$$

where ν_{in} is the collisional frequency between ions and neutrals. The quantum force acting on the ions is small owing to their large mass by comparison with electrons and positrons, and hence is neglected in Eq. (6). The perpendicular component of the velocity from Eq. (6) can be written as

$$\mathbf{v}_{i\perp}=\frac{c}{B_0}(\hat{\mathbf{z}}\times\nabla_\perp\phi)-\frac{c\nu_{in}}{\Omega_{ci}B_0}\nabla_\perp\phi-\frac{c}{B_0\Omega_{ci}}\partial_t\nabla_\perp\phi, \quad (7)$$

where the usual limit $\partial_t \ll \Omega_{ci}$ ($\Omega_{ci}=eB_0/cm_i$ is the ion cyclotron frequency) has been used for low frequency drift waves and ($\perp$) means the direction perpendicular to the magnetic field $\mathbf{B}_0$.

The parallel component of velocity from Eq. (6) is

$$\hat{A}v_{iz}=-\frac{e}{m_i}\partial_z\phi, \quad (8)$$

where $\hat{A}$ is an operator defined as

$$\hat{A}=(\partial_t+\nu_{in}+v_{iz}\partial_z).$$

Using the Poisson equation

$$\nabla^2\phi=-4\pi e(n_i+n_p-n_e), \quad (9)$$

and the perturbed ion number density from Eq. (9), we obtain

$$\left(\frac{\widetilde{n_i}}{n_{i_0}}\right)=\frac{3}{2}a_1\phi+b_1\phi^2-c_1\nabla^2\phi+d_1\nabla^2\phi. \quad (10)$$

Here, $a_1=e/k_BT_{Fe}[(n_{e_0}/n_{i_0})+(n_{p_0}/n_{i_0})(T_{Fe}/T_{Fp})]$, $b_1=3e^2/8k_B^2T_{Fe}^2[(n_{e_0}/n_{i_0})-(n_{p_0}/n_{i_0})(T_{Fe}/T_{Fp})^2]$, $c_1=1/4\pi en_{i_0}$, and $d_1=9e\hbar^2/16m_ek_B^2T_{Fe}^2[(n_{e_0}/n_{i_0})+(n_{p_0}/n_{i_0})(T_{Fe}/T_{Fp})^2]$, respectively.

The ion continuity equation is

$$\partial_tn_i+\nabla\cdot(n_i\mathbf{v}_i)=0. \quad (11)$$

Using Eqs. (7), (8), and (10) in Eq. (11), multiplying both sides by k_BT_{Fe}/e, we have

$$\frac{3}{2}a\partial_t\phi+b\partial_t\phi^2-\lambda_q^2\partial_t\nabla^2\phi+H_q^2\partial_t\nabla^2\phi-\varrho_s^2\partial_t\nabla_\perp^2\phi$$
$$-\varrho_s^2\nu_{in}\nabla_\perp^2\phi+\frac{3}{2}v_*\partial_y\phi+D_1\partial_y\phi^2+\frac{k_BT_{Fe}}{e}\partial_zv_{iz}=0, \quad (12)$$

where

$$a=[(n_{e_0}/n_{i_0})+(n_{p_0}/n_{i_0})(T_{Fe}/T_{Fp})],$$

$$b=3e/8k_BT_{Fe}[(n_{e_0}/n_{t_0})-(n_{p_0}/n_{i_0})(T_{Fe}/T_{Fp})^2],$$

$$\lambda_q=\sqrt{\lambda_{Fe}^2(n_{e_0}/n_{i_0})}$$

(λ_{Fe} is the electron Fermi wavelength given by $\sqrt{k_BT_{Fe}/4\pi e^2n_{e0}}$),

$$H_q=\sqrt{9\hbar^2/16m_ek_BT_{Fe}[(n_{e_0}/n_{i_0})+(n_{p_0}/n_{i_0})(T_{Fe}/T_{Fp})^2]}$$

is quantum diffraction length, $v_*=(2ck_BT_{Fe}/3eB_0)\kappa_{ni}$ is the drift velocity, $D_1=3c/4B_0[(n_{e_0}/n_{i_0})(\kappa_{ne}-\kappa_{T_{Fe}})+(T_{Fe}/T_{Fp})]$, $\kappa_{n_j}=|d_x\ln n_{j_0}|$ and $\kappa_{T_{Fj}}=|d_x\ln T_{F_{j0}}|$ are the inverse density and temperature gradient scale lengths for $j=e$ (electron) and p (positron), respectively. Also, $\kappa_{ni}=|d_x\ln n_{i_0}|=[(n_{e_0}/n_{i_0})\kappa_{ne}-(n_{p_0}/n_{i_0})\kappa_{np}]$ is the inverse density gradient scale length for ions.

Assuming $\partial_x \ll \partial_z < \partial_y$ and applying operator $\hat{A}$, Eq. (12) gives

$$\hat{A}\left\{\tfrac{3}{2}a\partial_t\phi+b\partial_t\phi^2-\lambda_q^2\partial_t\partial_y^2\phi+H_q^2\partial_t\partial_y^2\phi-\varrho_s^2\partial_t\partial_y^2\phi\right.$$
$$\left.-\varrho_s^2\nu_{in}\partial_y^2\phi+\tfrac{3}{2}v_*\partial_y\phi+D_1\partial_y\phi^2\right\}-c_s^2\partial_z^2\phi=0, \quad (13)$$

where $c_s=\sqrt{k_BT_{Fe}/m_i}$ is the quantum ion acoustic speed and $\varrho_s=\sqrt{k_BT_{Fe}/m_i\Omega_{ci}^2}$ is the ion Larmor radius at electron temperature. It is emphasized here that the term $b\partial_t\phi^2$ does not appear in Eq. (11) of Ref. 26 because the authors linearized the electron density and threw away the higher order contribution very early in their calculations, which later introduces nonlinearity in the system. Note that the coefficient of nonlinearity in Ref. 26 contains only the effects due to inhomogeneity and ignoring the density inhomogeneity would make nonlinearity vanish in their work. A similar error was committed in Refs. 26 and 38–40 where the authors discussed drift solitons and shocks in quantum and classical plasmas, respectively. The nonlinearity should not disappear with the disappearance of inhomogeneity as the KdV and KP equations are derived in homogeneous plasmas where the source of the nonlinearity is the convective derivative term. It is, therefore, imperative that the procedure given in this paper be followed to arrive at the correct equation. It is also worth mentioning that the nonlinearity coefficients obtained in Refs. 26 and 38–40 make, in fact, very small contributions as these contain the inhomogeneity term.

A. Case 1

Here we consider the case when collisions dominate, i.e., $\partial_t \ll \nu_{in}$, then Eq. (13) takes the form

$$\frac{3}{2}a\partial_t\phi + b\partial_t\phi^2 - \lambda_q^2\partial_t\partial_y^2\phi + H_q^2\partial_t\partial_y^2\phi - \varrho_s^2\partial_t\partial_y^2\phi - \nu_{in}\varrho_s^2\partial_y^2\phi + \frac{3}{2}v_*\partial_y\phi + D_1\partial_y\phi^2 - \frac{c_s^2}{\nu_{in}}\partial_z^2\phi = 0. \quad (13')$$

The last term of Eq. (13′) can be ignored because ν_{in} (which is large in this case) appears in the denominator and also due to the fact that perturbation in the parallel direction is weak. Thus, Eq. (13′) becomes

$$\tfrac{3}{2}a\partial_t\phi + b\partial_t\phi^2 - \lambda_q^2\partial_t\partial_y^2\phi + H_q^2\partial_t\partial_y^2\phi - \varrho_s^2\partial_t\partial_y^2\phi - \nu_{in}\varrho_s^2\partial_y^2\phi + \tfrac{3}{2}v_*\partial_y\phi + D_1\partial_y\phi^2 = 0. \quad (14)$$

B. Case 2

When $\partial_t \gg \nu_{in}$, Eq. (13) gives

$$\tfrac{3}{2}a\partial_t^2\phi + b\partial_t^2\phi^2 - \lambda_q^2\partial_t^2\partial_y^2\phi + H_q^2\partial_t^2\partial_y^2\phi - \varrho_s^2\partial_t^2\partial_y^2\phi - \nu_{in}\varrho_s^2\partial_t\partial_y^2\phi + \tfrac{3}{2}v_*\partial_t\partial_y\phi + D_1\partial_t\partial_y\phi^2 - c_s^2\partial_z^2\phi = 0. \quad (15)$$

III. LINEAR ANALYSIS

Upon linearizing Eq. (15) and assuming that the perturbation $\propto[ik_y y + ik_z z - i\omega t]$, the dispersion relation for the coupled quantum drift ion acoustic mode in dissipative quantum e-p-i plasma reads as

$$\omega = \frac{\left[\omega_* - \left(\frac{2}{3}\right)i\nu_{in}k_y^2\varrho_s^2\right] \pm \sqrt{\left[\omega_* - \left(\frac{2}{3}\right)i\nu_{in}k_y^2\varrho_s^2\right]^2 + \frac{8}{3}c_s^2k_z^2\left[a + \frac{2}{3}(\lambda_q^2 + \varrho_s^2 - H_q^2)k_y^2\right]}}{2\left[a + \frac{2}{3}(\lambda_q^2 + \varrho_s^2 - H_q^2)k_y^2\right]}, \quad (16)$$

where $\omega_* = v_* k_y$ is the drift frequency, ω is the wave frequency, k_y and k_z are the wave numbers, and $\left[a + \frac{2}{3}(\lambda_q^2 + \varrho_s^2 - H_q^2)k_y^2\right] > 0$ must hold for a finite solution. In the absence of positrons, i.e., $a=1$, Eq. (16) reduces to the same dispersion relation as obtained for an e-i quantum plasma.[37] From Eq. (16), separating the real and imaginary parts, we obtain

$$\omega_r = \frac{\omega_* + \sqrt{\omega_*^2 + \frac{8}{3}c_s^2k_z^2\left[a + \frac{2}{3}(\lambda_q^2 + \varrho_s^2 - H_q^2)k_y^2\right]}}{2\left[a + \frac{2}{3}(\lambda_q^2 + \varrho_s^2 - H_q^2)k_y^2\right]}, \quad (17)$$

$$\omega_i = \frac{\frac{2}{3}\nu_{in}\varrho_s^2k_y^2 + \dfrac{\frac{2}{3}\omega_*\nu_{in}\varrho_s^2k_y^2}{\sqrt{\omega_*^2 + \frac{8}{3}c_s^2k_z^2\left[a + \frac{2}{3}(k_q^2 + \varrho_s^2 - H_q^2)k_y^2\right]}}}{2\left[a + \frac{2}{3}(\lambda_q^2 + \varrho_s^2 - H_q^2)k_y^2\right]}, \quad (18)$$

where ω_r and ω_i are the real and imaginary frequencies, $k_y = k\cos\theta$, and $k_z = k\sin\theta$. It can be seen from Eqs. (17) and (18) that for small k, the numerator dominates since it is proportional to k and, hence, the corresponding increase in ω (real and imaginary). However, for large k, the denominator increases resulting in a decrease in ω (real and imaginary). Figures 1 and 2 show the variation in real and imaginary frequencies (related to damping) of the coupled quantum drift ion acoustic mode as a function of obliqueness. It is found that the real frequencies enhance, whereas the imaginary frequencies decrease with the increase in the obliqueness angle θ. Figures 3 and 4 show the variation in real and imaginary frequencies as a function of positron concentration. By increasing the positron concentration, quantum effects become pronounced, resulting in an increase in real and imaginary frequencies for small k. The variation in the real frequency and the damping rate could similarly be found by varying the other plasma parameters.

In the absence of collisions between ions and neutral particles, i.e., $\nu_{in}=0$, Eq. (16) can be written as

$$\omega = \frac{\omega_* \pm \sqrt{\omega_* + \frac{8}{3}c_s^2k_z^2\left[a + \frac{2}{3}(\lambda_q^2 + \varrho_s^2 - H_q^2)k_y^2\right]}}{2\left[a + \frac{2}{3}(\lambda_q^2 + \varrho_s^2 + H_q^2)k_y^2\right]}. \quad (19)$$

In the absence of inhomogeneity in density and temperature, i.e., $\omega_*=0$, Eq. (16) can be written as

$$\omega = \frac{\pm\sqrt{\frac{2}{3}}c_s k_z}{\sqrt{\left[a + \frac{2}{3}(\lambda_q^2 + \varrho_s^2 - H_q^2)k_y^2\right]}}. \quad (20)$$

It is evident from Eqs. (16)–(18) that quantum corrections affect the dispersion characteristics of the coupled quantum ion acoustic and drift mode in dissipative quantum e-p-i plasma.

IV. DERIVATION OF KdVB

In order to find the localized solution, let us choose a coordinate η in the moving frame such that $\eta = \chi\,(y - ut)$, where χ is nonlinear wave number and u is the velocity of the nonlinear structure moving with the frame. Equation (14) in the transformed frame can be written as

$$-S_1 d_\eta\phi + S_2 d_\eta\phi^2 + S_3\chi^2 d_\eta^3\phi - S_4\chi d_\eta^2\phi = 0, \quad (21)$$

where $S_1 = \frac{3}{2}(a - v_*/u)$, $S_2 = -(b - D_1/u)$, $S_3 = (\lambda_q^2 + \varrho_s^2 - H_q^2)$, and $S_4 = \varrho_s^2\nu_{in}/u$. Equation (21) can further be simplified to obtain

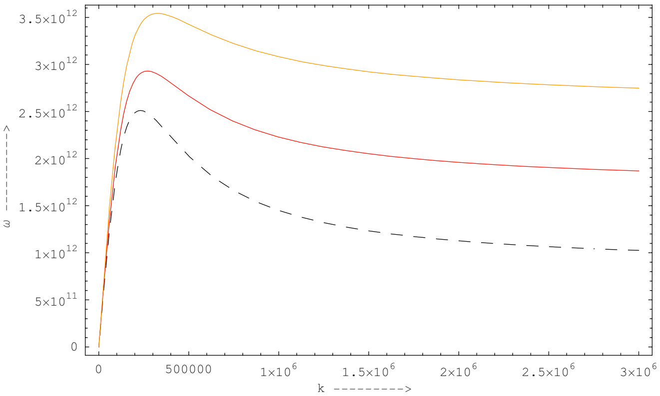

FIG. 1. (Color online) Variation in the real frequency of the coupled drift ion acoustic wave with the obliqueness angle θ. Other parameters are $n_{e_0}=1.9\times 10^{27}$ cm^{-3}, $n_{i_0}=1.6\times 10^{27}$ cm^{-3}, $n_{p_0}=3\times 10^{26}$ cm^{-3}, $B_0=10^9$ G, and $\theta=5°,10°,15°$.

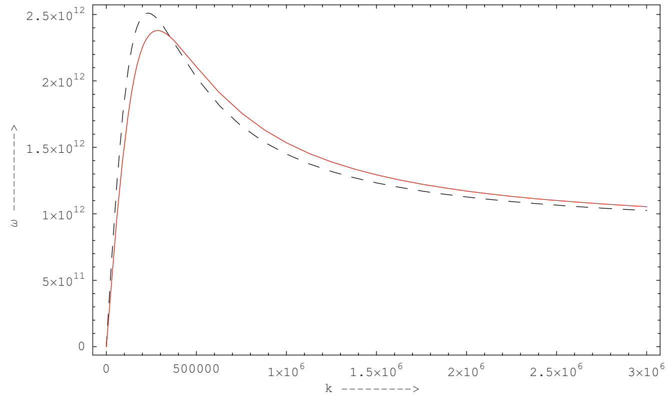

FIG. 3. (Color online) Variation in the real frequency of the coupled drift ion acoustic wave for increasing positron concentration, i.e., $n_{p_0}=3\times 10^{26}$ cm^{-3} (dashed line) and $n_{p_0}=7\times 10^{26}$ cm^{-3} (solid line). Other parameters are $B_0=10^9$ G and $\nu_{in}=10^{10}$ s^{-1}.

$$-d_\eta\phi + Ad_\eta\phi^2 + B\chi^2 d_\eta^3\phi - C\chi d_\eta^2\phi = 0, \quad (22)$$

where $A=S_2/S_1$, $B=S_3/S_1$, and $C=S_4/S_1$.

There are numerous methods to solve the nonlinear partial differential equations (NLPDEs), for instance, inverse scattering method,[41] Hirota bilinear formalism.[42] Backlund transformation,[43] tangent hyperbolic (tanh) method,[44] etc. However, when the partial differential equation in a system is formed by the combined effect of dispersion and dissipation, the most convenient and efficient method to solve such NLPDE is tanh.[45] Therefore, using tanh method, we arrive at the following solution of Eq. (22):

$$\phi(\eta) = \frac{25B+3C^2}{50AB} - \frac{3C^2}{25AB}\tanh(\eta) - \frac{3C^2}{50AB}\tanh^2(\eta), \quad (23)$$

where $\eta=\varkappa(y-ut+\alpha z)=C/10B(y-ut+\alpha z)$ and the value of C for which the above solution satisfies the boundary conditions turns out to be $\sqrt{25B/6}$. The width of the shock structure can be found by taking the inverse of $\varkappa=|C/10B|$. It should be mentioned here that the solution of KdVB presented in Ref. 26 is wrong as it does not satisfy the KdVB [i.e., Eq. (14) in Ref. 26]. Equation (23) presents the correct solution of the quantum KdVB equation in an electron-positron-ion plasma.

V. DERIVATION OF KPB

For the localized solution, we assume a new coordinate η in the moving frame such that $\eta=\chi(y+\alpha z-ut)$, where α is the angle between wavefront normal and xy-plane. Equation (15) in the transformed frame and can be written as

$$d_\eta[A_1 d_\eta\phi + A_2 d_\eta\phi^2 + A_3\chi^2 d_\eta^3\phi + A_4\chi d_\eta^2\phi] + \alpha^2 A_5 d_\eta^2\phi = 0, \quad (24)$$

where $A_1=\frac{3}{2}(a-v_*/u)$, $A_2=(b-D_1/u)$, $A_3=-(\lambda_q^2+\varrho_s^2-H_q^2)$, $A_4=\nu_{in}\varrho_s^2/u$, and $A_5=-c_s^2/u^2$. Equation (24) can be simplified further to obtain

$$d_\eta[d_\eta\phi + Ad_\eta\phi^2 + B\chi^2 d_\eta^3\phi + C\chi d_\eta^2\phi] + \alpha^2 D d_\eta^2\phi = 0, \quad (25)$$

where $A=A_2/A_1$, $B=A_3/A_1$, $C=A_1/A_1$, and $D=A_5/A_1$. Again, employing the tanh method, we obtain the following solution for the quantum KPB [Eq. (25)]:

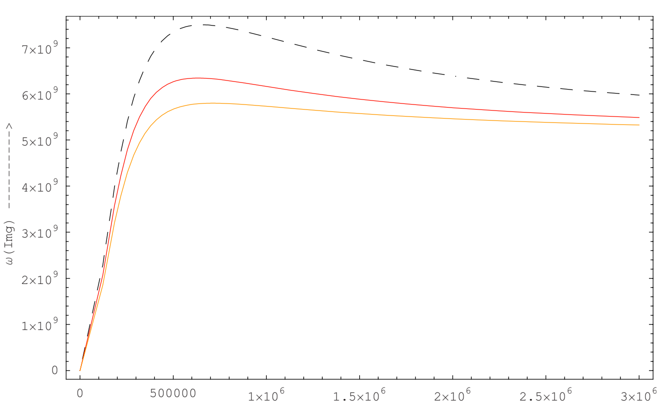

FIG. 2. (Color online) Variation in the imaginary frequency of the coupled drift ion acoustic wave with the obliqueness angle θ. Other parameters are $n_{e_0}=1.9\times 10^{27}$ cm^{-3}, $n_{i_0}=1.6\times 10^{27}$ cm^{-3}, $n_{p_0}=3\times 10^{26}$ cm^{-3}, $B_0=10^9$ G, and $\theta=5°,10°,15°$.

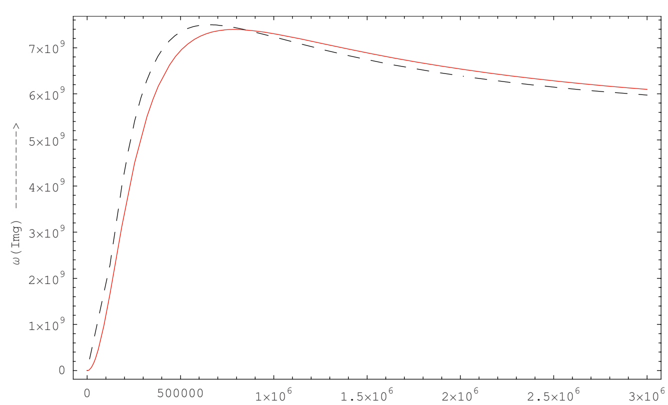

FIG. 4. (Color online) Variation in the imaginary frequency of the coupled drift ion acoustic wave for increasing positron concentration, i.e., $n_{p_0}=3\times 10^{26}$ cm^{-3} (dashed line) and $n_{p_0}=7\times 10^{26}$ cm^{-3} (solid line). Other parameters are $B_0=10^9$ G and $\nu_{in}=10^{10}$ s^{-1}.

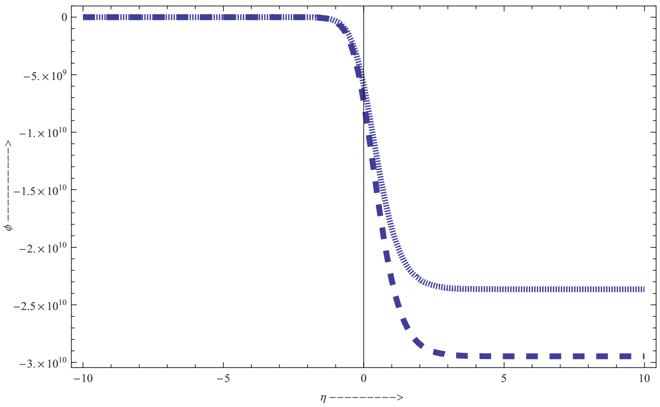

FIG. 5. (Color online) Variation in the electrostatic potential ϕ for different values of positron concentration, i.e., $n_{p_0}=1\times10^{26}$ cm^{-3} (solid line) and $n_{p_0}=3\times10^{26}$ cm^{-3} (dashed line). Other parameters are $n_{e_0}=1.9\times10^{27}$ cm^{-3}, $B_0=10^9$ G, and $\nu_{in}=10^{10}$ s^{-1}.

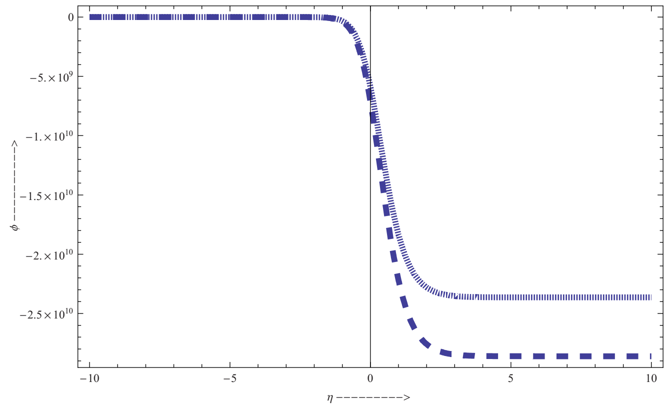

FIG. 6. (Color online) Variation in the electrostatic potential ϕ for different values of collision frequency, i.e., $\nu_{in}=1.1\times10^{10}$ s^{-1} (dashed line) and $\nu_{in}=10^{10}$ s^{-1} (solid line). Other parameters are $n_{e_0}=1.9\times10^{27}$ cm^{-3} and $B_0=10^9$ G.

$$\phi(\eta)=\frac{-25B+3C^2-25\alpha^2BD}{50AB}+\frac{3C^2}{25AB}\tanh(\eta)-\frac{3C^2}{50AB}\tanh^2(\eta), \tag{26}$$

where the value of α for which the above solution satisfies the boundary condition turns out to be $\sqrt{(6C^2-25B)/25BD}$. The width of the shock structure can be found by taking the inverse of $\varkappa=|C/10B|$. Note that the second term that involves tanh term in Eq. (26) is responsible for the shocklike structure as it destroys the balance between dispersion and nonlinearity unlike the ordinary KP which has a sech^2 type solution and admits solitary wave solution.

VI. STABILITY ANALYSIS

In order to check the stability of the KPB, we proceed as follows. Integrate Eq. (25) twice to obtain

$$-Ay^2-B\chi^2d_\eta^2y+C\chi d_\eta y+(1-\alpha^2D)y=0, \tag{27}$$

where $A=A_2/A_1$, $B=-A_3/A_1$, $C=A_4/A_1$, and $D=-A_5/A_1$, $y=\phi$. Appropriate boundary conditions are imposed, namely, $y\to0$, $d_\eta y\to0$, $d_\eta^2y\to0$ at $\eta\to-\infty$ to investigate the asymptotic behavior of Eq. (27) by linearizing it with respect to y.[46] Simplifying, we get

$$-B\chi^2d_\eta^2y+C\chi d_\eta y-(1-\alpha^2D)y=0. \tag{28}$$

The solutions of Eq. (28) are proportional to $\exp(W\eta)$, where $W=5[1\mp\sqrt{1-4B(1-\alpha^2D)/C^2}]$. From Eq. (28), it is clear that the quantum corrections appear in the dispersion coefficient B. Also note that there will be a stable shock if $4B(1-\alpha^2D)/C^2<1$, else there will be an oscillatory shock.

VII. RESULTS AND DISCUSSION

In this section, we numerically investigate the dependence of wave potential of the quantum drift ion acoustic shock wave on the quantum Bohm potential, collision frequency, and the ratio of drift to shock velocity in the comoving frame, i.e., v_*/u in dense e-p-i plasmas. In high density plasmas found in dense astrophysical objects such as neutron stars and white dwarfs, the plasma densities are enormous and quantum effects may be important. For illustration, parameters are chosen which are representatives of the plasma in dense astrophysical bodies, i.e., $n_o\sim10^{26}-10^{28}$ cm^{-3} and $B_o\sim10^9-10^{11}$ G.[26] Graphical analysis of ion acoustic drift shock profile given by Eq. (26) is presented by plotting the potential ϕ against different parameters affecting the wave. In Fig. 5, the variation in the wave potential with the increasing positron concentration is shown. It is found that increasing the positron concentration decreases the strength of the shock. It is also seen from Eq. (26) that the expression of the quantum Bohm potential involves density, and therefore the variation in density indirectly represents the change in the wave potential with the quantum Bohm potential term.

Figure 6 shows the effect of increasing collision frequency on the wave potential. It is found that the increasing collision frequency decreases the shock strength of the drift acoustic shock wave. Finally, Fig. 7 explores how the ratio of drift to shock velocity in the comoving frame, v_*/u, affects the shock structure. In this regard, two cases are considered, i.e., $v_*\gtrless u$. It is found that for $u>v_*$, the shock strength

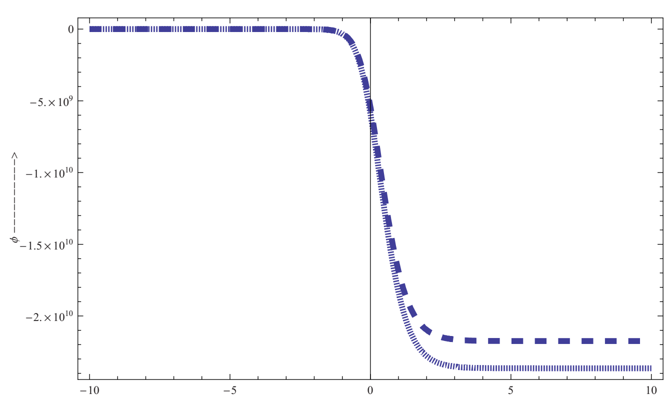

FIG. 7. (Color online) Variation in the electrostatic potential ϕ for different values of v_*/u, i.e., $u>v_*$ (solid line) and $v_*>u$ (dashed line). Other parameters are $n_{e_0}=1.9\times10^{27}$ cm^{-3}, $B_0=10^9$ G, and $\nu_{in}=10^{10}$ s^{-1}.

decreases, whereas it increases for the case when $u<v_*$. This owes to the change in the sign of the nonlinearity coefficient, A, appearing in Eq. (26).

VIII. CONCLUSION

Linear and nonlinear propagation characteristics of drift ion acoustic shock waves in a two-dimensional (2D) inhomogeneous e-p-i quantum magnetoplasma are studied here using the QHD model. In this regard, a quantum KPB equation for an inhomogeneous plasma is derived using the drift approximation. It is found that the ion acoustic mode couples with the drift wave if the parallel motion of ions is taken into account. Discrepancies in the earlier works have also been pointed out and a correct theoretical framework is presented to study the one-dimensional (1D) as well as the 2D propagation of shock waves in an inhomogeneous quantum plasma. Furthermore, the solutions of KdVB and KPB equations are presented using the tangent hyperbolic (tanh) method. The effects of quantum Bohm potential (via the varying positron concentration), collision frequency, and the ratio of drift to shock velocity in the comoving frame on the shock profiles are numerically illustrated in Figs. 5–7. It is found that increasing the positron number density and collision frequency decreases the shock strength. Finally, it is found that when the localized structure propagates with velocity greater than the drift velocity, the quantum drift ion acoustic shock strength decreases, whereas it enhances when the localized structure propagates with velocity less than the drift velocity. The present study may be relevant to the study of dense astrophysical environments such as neutron stars and white dwarfs where the quantum effects are expected to dominate.

ACKNOWLEDGMENTS

One of the authors (S.K.) would like to thank Salam Chair, Government College University, Lahore, Pakistan, for providing the financial assistance to carry out this research work.

[1] A. Markowich, C. Ringhofer, and C. Schmeiser, *Semiconductor Equations* (Springer, Vienna, 1990).
[2] M. Opher, L. O. Silva, D. E. Dauger, V. K. Decyk, and J. M. Dawson, Phys. Plasmas **8**, 2454 (2001).
[3] Y. D. Jung, Phys. Plasmas **8**, 3842 (2001).
[4] M. Marklund and P. K. Shukla, Rev. Mod. Phys. **78**, 591 (2006).
[5] P. K. Shukla and S. Ali, Phys. Plasmas **12**, 114502 (2005).
[6] W. Masood, A. Mushtaq, and R. Khan, Phys. Plasmas **14**, 123702 (2007).
[7] S. A. Khan, W. Masood, and M. Siddiq, Phys. Plasmas **16**, 013701 (2009).
[8] G. Manfredi, Fields Inst. Commun. **46**, 263 (2005).
[9] W. Masood and A. Mushtaq, Phys. Lett. A **372**, 4283 (2008).
[10] S. Ali, W. M. Moslem, P. K. Shukla, and R. Schlickeiser, Phys. Plasmas **14**, 082307 (2007).
[11] W. F. El-Taibany and M. Wadati, Phys. Plasmas **14**, 42302 (2007).
[12] P. K. Shukla and L. Stenflo, Phys. Lett. A **357**, 229 (2006).
[13] Z. Wu, H. Ren, J. Cao, and P. K. Chu, Phys. Plasmas **15**, 082103 (2008).
[14] W. Masood, A. M. Mirza, and S. Nargis, Phys. Plasmas **15**, 122305 (2008).
[15] F. B. Rizatto, J. Plasma Phys. **40**, 288 (1988).
[16] M. Y. Yu, Astrophys. Space Sci. **177**, 203 (1985).
[17] H. R. Mille and P. Witta, *Active Galactic Nuclei* (Springer, Berlin, 1987), p. 202.
[18] F. C. Michel, Rev. Mod. Phys. **54**, 1 (1982).
[19] F. C. Michel, *Theory of Neutron Star Magnetosphere* (Chicago University Press, Chicago, 1991).
[20] V. Berezhiani, D. D. Tskhakaya, and P. K. Shukla, Phys. Rev. A **46**, 6608 (1992).
[21] W. Misner, K. Thorne, and J. A. Wheeler, *Gravitation* (Freeman, San Francisco, 1973), p. 763.
[22] M. L. Burns, in *Positron-Electron Pairs in Astrophysics*, edited by M. L. Burns, A. K. Harding, and R. Ramaty (American Institute of Physics, Melville, NY, 1983).
[23] S. A. Khan and W. Masood, Phys. Plasmas **15**, 062301 (2008).
[24] W. Masood, A. M. Mirza, and M. Hanif, Phys. Plasmas **15**, 072106 (2008).
[25] R. Sabry, W. Moslem, and P. K. Shukla, Eur. Phys. J. D **51**, 233 (2009).
[26] Q. Haque, S. Mahmood, and A. Mushtaq, Phys. Plasmas **15**, 082315 (2008).
[27] H. Ren, Z. Wu, J. Cao, and P. K. Chu, J. Phys. A **41**, 115501 (2008).
[28] B. Sahu and R. Roychoudhury, Phys. Plasmas **14**, 072310 (2007).
[29] A. A. Mamun and P. K. Shukla, Phys. Plasmas **9**, 1468 (2002).
[30] J.-K. Xue, Phys. Plasmas **10**, 4893 (2003).
[31] P. K. Shukla and A. A. Mamun, New J. Phys. **5**, 17 (2003).
[32] S. V. Vladimirov and M. Y. Yu, Phys. Rev. E **48**, 2136 (1993).
[33] S. V. Vladimirov and M. Y. Yu, Phys. Rev. E **49**, 1569 (1994).
[34] J.-K. Xue, Phys. Plasmas **10**, 3430 (2003).
[35] J.-K. Xue, Phys. Lett. A **314**, 479 (2003).
[36] L. Landau and E. M. Lifshitz, *Statistical Physics* (Oxford University Press, Oxford, 1980), Pt. 1, p. 167.
[37] W. Masood, S. Karim, H. A. Shah, and M. Siddiq, Phys. Plasmas **16**, 042108 (2009).
[38] Q. Haque and S. Mahmood, Phys. Plasmas **15**, 034501 (2008).
[39] H. Saleem, Phys. Plasmas **13**, 034503 (2006).
[40] H. Saleem and N. Batool, Phys. Plasmas **16**, 022302 (2009).
[41] M. J. Ablowitz and P. A. Clarkson, *Solitons, Nonlinear Evolution Equations and Inverse Scattering* (Cambridge University Press, Cambridge, 1991).
[42] R. Hirota, Phys. Rev. Lett. **27**, 1192 (1971).
[43] M. R. Miura, *Backlund Transformation* (Springer-Verlag, Berlin, 1978).
[44] W. Malfliet, Am. J. Phys. **60**, 650 (1992).
[45] W. Malfliet, J. Comput. Appl. Math. **164**, 529 (2004).
[46] V. I. Karpman, *Nonlinear Waves in Dispersive Media* (Pergamon, Oxford, 1975).